J Supercond Nov Magn (2017) 30:2233–2238
DOI 10.1007/s10948-017-4039-z

ORIGINAL PAPER

Study of Magnetocaloric Effect and Magnetic Phase Transition of Electron-Doped $La_{0.9}Sb_{0.1}MnO_3$ Manganite

Quan-shui Meng[1] · Li-an Han[1] · Lin Chang[1] · Jing Yang[1] · Zheng-xin Yan[1]

Received: 15 December 2016 / Accepted: 24 February 2017 / Published online: 7 March 2017

Abstract An electron-doped $La_{0.9}Sb_{0.1}MnO_3$ manganite was prepared by a sol-gel method, and its magnetocaloric effect and magnetic phase transition (MPT) have been systematically studied. The X-ray diffraction pattern is consistent with the rhombohedral lattice structure ($R\bar{3}C$ space group). This sample shows a ferromagnetic order at T_C = 248 K. A maximum magnetic entropy change ($-\Delta S_M{}^{max}$) of 4.79 J kg^{-1} K^{-1} and a relative cooling power (RCP) of 258.15 J kg^{-1} are observed at a magnetic field change of 5 T. It is found that the values of $-\Delta S_M{}^{max}$ are comparable to some hole-doped manganese compounds. Nevertheless, RCP values of $La_{0.9}Sb_{0.1}MnO_3$ are higher than those of some hole-doped manganites under the same field change, which is very beneficial for designing the magnetic refrigeration materials in engineering. Furthermore, Arrott plots reveal a second-order MPT for $La_{0.9}Sb_{0.1}MnO_3$, which is also confirmed by Franco's universal curves. In addition, the experimental observed $-\Delta S_M$ follows Lauder's mean-field theory very well, which demonstrates that the magneto-elastic and magneto-electronic couplings have a crucial importance on the magnetic entropy change of $La_{0.9}Sb_{0.1}MnO_3$ manganite.

Keywords Magnetocaloric effect · Magnetic phase transition · Landau's theory · Electron-doped manganite

✉ Li-an Han
hanlianvivian@sohu.com

[1] Department of Applied Physics, Xi'an University of Science and Technology, Xi'an 710054, China

1 Introduction

Mixed-valence manganites of the type $La_{1-x}AE_xMnO_3$ (AE = Li, Na, K or Sr, Ca, Ba, etc.) with the perovskite structure have been intensively investigated for more than 60 years because of their noticeable physical properties [1–3] (colossal magnetoresistance (CMR) effect, ferromagnetic-paramagnetic transition, metal-insulator transition, magnetocaloric effect, etc.) and potential technological applications in spintronic devices [4–6]. In the recent past, many studies on the substitution of tetravalent ions (Te^{4+}, Zr^{4+}, Sn^{4+}, and Hf^{4+}) [7–10] or pentavalent ions (Sb^{5+}) [11] for trivalent La^{3+} in parent compound $LaMnO_3$ reveal that magnetic, transport, and magnetoresistive properties similar to those of the monovalent and/or divalent ions doped (also named as hole-doped) manganese oxides are also observed in the case of these tetravalent and/or pentavalent ions substituted (named electron-doped) manganites. In order to explain the same physical properties in electron-doped manganese compounds, many researchers [7–10] have believed that the CMR effect and FM-PM transition can be explained via the double-exchange interaction between Mn^{2+} and Mn^{3+}, instead of double-exchange interaction between Mn^{3+} and Mn^{4+} ions as in hole-doped manganites [12].

Aside from the CMR effect, more recently, a large magnetocaloric effect (MCE) was also observed in electron-doped manganites and captured tremendous interest. Yang et al. [13] reported that the magnetic entropy change (MEC) of $La_{0.9}Te_{0.1}MnO_3$ was 1.85 J kg^{-1} K^{-1} for a magnetic field change of 1.5 T at 252 K, and the corresponding relative cooling power (RCP) of this sample was 541 mJ cm^{-3}. Mahato et al. [14] studied MCE properties of nanocrystalline $La_{0.7}Te_{0.3}MnO_3$ and found a larger change

in magnetic entropy value, namely, 12.5 J kg^{-1} K^{-1} under $\mu_0 \Delta H = 5$ T. Shelke et al. [15] studied the MCE of electron-doped manganites $La_{1-x}Zr_xMnO_3$ ($x = 0.05$, 0.10, and 0.15) and found that the MEC and RCP of these compounds were higher than those of some hole-doped manganites.

Up to now, most of the pervious works have been focused on the magnetic and transport properties of electron-doped $La_{0.9}Sb_{0.1}MnO_3$ [16–18]. But the research on the MEC of $La_{0.9}Sb_{0.1}MnO_3$ compound is still lacking. The study of $La_{0.9}Sb_{0.1}MnO_3$ will offer a complementary understanding of the MCE in the ABO_3-type perovskite manganites and may provide a new opportunity for developing highly efficient and environmentally friendly cooling devices. In this paper, we extend our investigation to the system of $La_{0.9}Sb_{0.1}MnO_3$ for studying its MCE and magnetic phase transition (MPT).

2 Experimental

Polycrystalline $La_{0.9}Sb_{0.1}MnO_3$ was synthesized by sol-gel route with stoichiometric compositions of highly pure La_2O_3 (99.95 %) powders, Sb_2O_5 (99.9 %) powders and $Mn(NO_3)_2$ (50 %) solution as starting materials. The precursors were dissolved in diluted nitric acid in which an excess of citric acid was added, followed with continuous stirring for about 10 h. After all reactants were completely dissolved, the solution was heated on a water bath at 353 K leading to the formation of a brown gel. The gel was dried at 373 K in an oven and then preheated at 873 K to remove the remaining organic and decompose the nitrates of the gel. The obtained black powders were mixed, ground, and sintered at 1473 K for 12 h. This step mentioned above was repeated three times for a better chemical homogeneity. Finally, the furnace was slowly cooled down to room temperature.

The phase structure of $La_{0.9}Sb_{0.1}MnO_3$ was performed by x-ray diffraction (XRD) using θ–2θ scans with Cu Kα radiation. Temperature and magnetic field-dependent magnetization measurements were carried out by means of a quantum design superconducting quantum interference device.

3 Results and Discussion

3.1 Structure

The phase purity and homogeneity of the polycrystalline $La_{0.9}Sb_{0.1}MnO_3$ sample was determined with a powder X-ray diffractometer. The XRD pattern (Fig. 1) of this sample confirms its single-phase nature and rhombohedral structure with the space group of $R\bar{3}C$ ($Z = 6$).

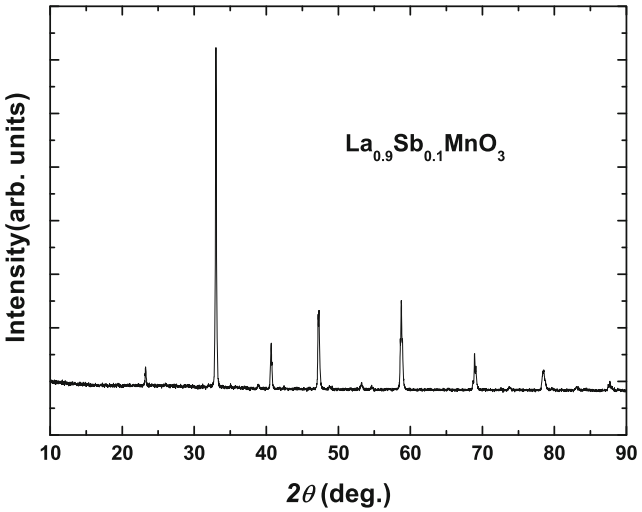

Fig. 1 XRD pattern of $La_{0.9}Sb_{0.1}MnO_3$ manganite

3.2 Magnetic Properties

Figure 2 displays the temperature dependence of the thermal magnetization (M-T) of the $La_{0.9}Sb_{0.1}MnO_3$ sample in the zero-field-cooled (ZFC) mode under an external field of 0.1 T, which shows a sharp paramagnetic-ferromagnetic (PM-FM) transition at Curie temperature (T_C). Usually, T_C can be estimated from the dM/dT versus T plot and corresponds to the minimum value [19], as shown on the right hand of Fig. 2. The sample exhibits a $T_C$value of about 248 K, in good agreement with the literature [16].

3.3 Magnetocaloric Effect

In order to calculate the MCE of the $La_{0.9}Sb_{0.1}MnO_3$ compound, a set of isothermal magnetization curves were recorded in the temperature range of 192–288 K with a step

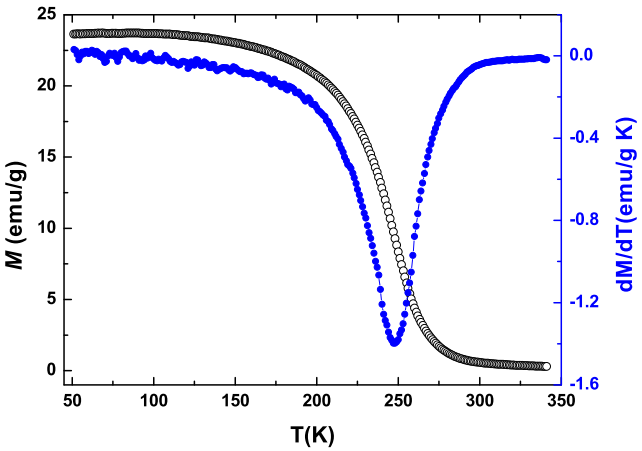

Fig. 2 *Left side* $M(T)$ curve in a magnetic field of 0.1 T for $La_{0.9}Sb_{0.1}MnO_3$; *right side* plot of *dM/dT* versus T

of 3 k up to a maximum applied field of 5 T and are displayed in Fig. 3. M-H curves of the compound exhibit a rapid increase at lower fields and get saturated at higher fields for all the temperatures measured, which indicate a typical FM behavior below T_C [20]; the $M-\mu_0 H$ data show a linear behavior as typical in the PM state at temperatures above T_C [21].

Magnetic refrigeration (MR) operates on the basis of MCE and is a desirable and green cooling technology owing to the fact that it has higher energy efficiency and less impact on the environment than conventional technology based on the gas compression-expansion cycle [22]. The MCE can be characterized by an isothermal MEC or an adiabatic temperature change of a material upon the application of a magnetic field. MEC can be calculated as [23]

$$|\Delta S_M(T,H)| = |S_M(T,H) - S_M(T,0)| = \int_0^{H_{\max}} \left(\frac{\partial S}{\partial H}\right)_T \mu_0 dH \quad (1)$$

Using Maxwell's thermodynamic relation

$$\left(\frac{\partial M}{\partial T}\right)_H = \left(\frac{\partial S}{\partial H}\right)_T \quad (2)$$

one can deduce the following expression [23]:

$$|\Delta S_M(T,H)| = \int_0^{H_{\max}} \left(\frac{\partial M}{\partial T}\right)_H \mu_0 dH \quad (3)$$

In practice, the MEC ($-\Delta S_M$) can be estimated from the isothermal magnetization measured with a small interval, where MEC can be approximated as [23]

$$\Delta S_M = \mu_0 \sum_i \frac{M_i - M_{i+1}}{T_i - T_{i+1}} \Delta H_i \quad (4)$$

where M_i and M_{i+1} are magnetizations at T_i and T_{i+1}, respectively, under the external magnetic field $\mu_0 \Delta H_i$.

Figure 4 shows the temperature dependencies of the MEC for the $La_{0.9}Sb_{0.1}MnO_3$ compound in magnetic field intervals ranging from 1 to 5 T. The values for $-\Delta S_M$ are positive in the whole temperature range. For each magnetic field, the $-\Delta S_M$ curve grows up a maximum value ($-\Delta S_M{}^{\max}$) close to the T_C, where the change of magnetization with temperature is strong. With $\mu_0 \Delta H = 1$, 2, 3, 4, and 5 T, the $-\Delta S_M{}^{\max}$ is about 1.65, 2.66, 3.50, 4.18, and 4.79 J kg^{-1} K^{-1}, respectively.

For the application of magnetic refrigeration, the relative cooling power (RCP) is another meaningful parameter in selecting a proper potential for magnetic refrigerant, which can be represented by the amount of heat transferred between the hot and cold sinks in the ideal refrigeration cycle. According to the definition of RCP suggested by Gschneidner et al. [24]:

$$RCP = -\Delta S_M^{\max}(T,H) \times \delta T_{FWHM} \quad (5)$$

where δT_{FWHM} is the full-width temperature span of the $-\Delta S_M$ vs. T curve at its half maximum. The RCP values of $La_{0.9}Sb_{0.1}MnO_3$ under magnetic fields of $\mu_0 \Delta H = 1$, 2, 3, 4, and 5 T are found to be 43.37, 84.32, 139.21, 191.67, and 258.15 J kg^{-1}, respectively. The RCP parameter is considered to be a suitable factor for comparing different MR materials. To assess the applicability of electron-doped $La_{0.9}Sb_{0.1}MnO_3$ manganite as a magnetic refrigerant, $-\Delta S_M{}^{\max}$, RCP values, and other magnetic parameters for $La_{0.9}Sb_{0.1}MnO_3$ as well as other samples are collected in Table 1. Obviously, $La_{0.9}Sb_{0.1}MnO_3$ presents moderate values of $-\Delta S_M{}^{\max}$ among the listed hole- and electron-doped manganites. However, the RCP value of $La_{0.9}Sb_{0.1}MnO_3$ is higher than that of some hole-doped ABO_3-type manganese compounds under the same field change, which is beneficial to magnetic cooling. Though the values of $-\Delta S_M{}^{\max}$ and RCP for the present sample are smaller than

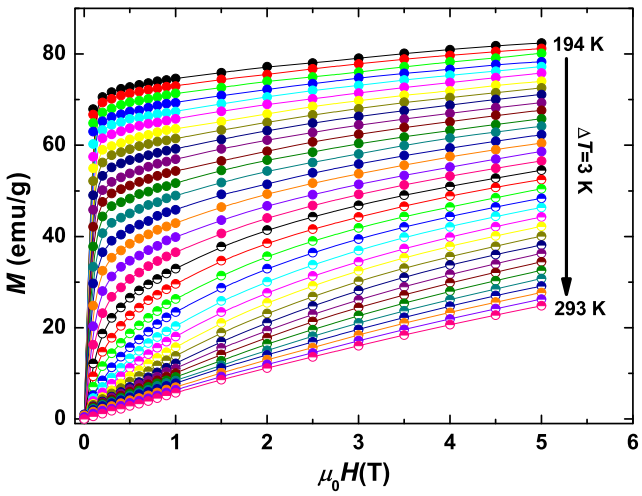

Fig. 3 Isothermal $M-\mu_0 H$ curves for $La_{0.9}Sb_{0.1}MnO_3$ between 194 and 293 K in the ΔT of 3 K

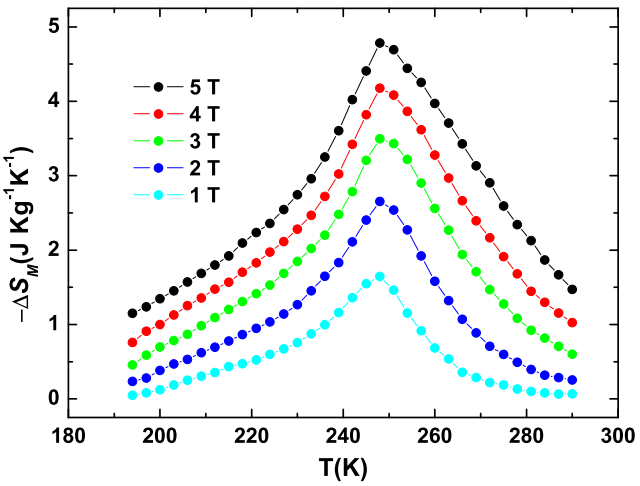

Fig. 4 Temperature dependence of $-\Delta S_M$ at different applied fields for $La_{0.9}Sb_{0.1}MnO_3$

Table 1 Summary of magnetocaloric properties for $La_{0.9}Sb_{0.1}MnO_3$ manganites. The present results of $La_{0.9}Sb_{0.1}MnO_3$ are compared with some of ABO3-type manganites and pure Gd

Composition	T_C (K)	$\mu_0\Delta H$ (T)	$-\Delta S_M{}^{max}$ (J kg^{-1}K^{-1})	RCP (J kg^{-1})	Source of data
$La_{0.9}Sb_{0.1}MnO_3$	248	5	4.79	258.15	Present work
$La_{0.9}Sb_{0.1}MnO_3$	248	2	2.66	84.32	Present work
$La_{0.9}Te_{0.1}MnO_3$	252	1.5	1.85	–	[12]
$La_{0.7}Te_{0.3}MnO_3$	280	5	12.5	–	[13]
$La_{0.85}Zr_{0.15}MnO_3$	180	5	2.08	142.50	[14]
$La_{0.67}Sr_{0.33}MnO_3$	370	5	5.15	252	[25]
$La_{0.67}Ba_{0.33}MnO_3$	292	5	1.48	161	[26]
$La_{0.67}Pb_{0.33}MnO_3$	352	5	0.96	48	[27]
$La_{0.94}Bi_{0.06}MnO_3$	209	1	1.58	44.86	[28]
$La_{0.7}Ca_{0.3}MnO_3$	252	5	8.15	197	[29]
Gd	293	5	9.5	410	[30]

those of some typical magnetic refrigerant materials such as pure Gd and $Gd_5(Si_{1-x}Ge_x)_4$, $La_{0.9}Sb_{0.1}MnO_3$ polycrystalline has many advantages including low production cost, negligible magnetic hysteresis, and high resistivity. Therefore, $La_{0.9}Sb_{0.1}MnO_3$ polycrystalline could be a promising magnetocaloric material.

3.4 Magnetic Phase Transition

It is generally accepted that the order of MPT can be judged with Banerjee's criterion [31]. According to this criterion, the negative slopes or inflection points in the Arrott plots ($\mu_0 H/M$ versus M^2 curves) are related to the first-order MPT, while the positive slopes and linear behavior near T_C often mean that the MPT belongs to the second order. In order to identify the nature of the MPT in $La_{0.9}Sb_{0.1}MnO_3$, the M-$\mu_0 H$ curves were converted into Arrott plots at some temperatures, as shown in Fig. 5. Neither a negative slope nor inflections over the whole field intervals is found near T_C in the Arrott plots, indicating the second-order feature of the MPT.

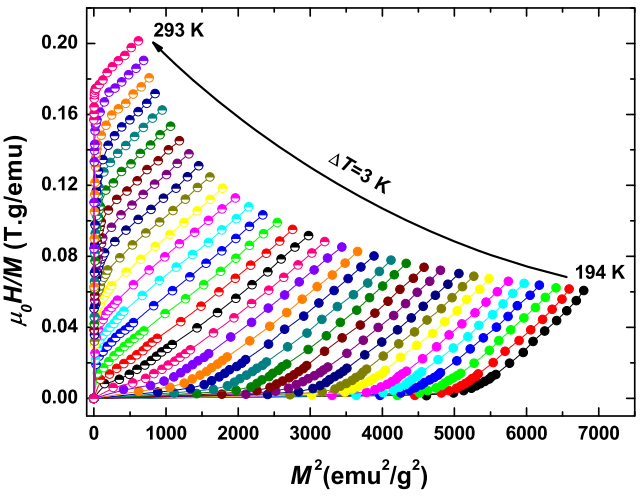

Fig. 5 A set of typical $\mu_0 H/M$ versus M^2 curves for $La_{0.9}Sb_{0.1}MnO_3$ at different temperatures close to T_C

Franco and co-workers have introduced a new method to discriminate the order of MPT [32, 33]. They suggested that the order of FM-PM transition can be conveniently distinguished with the re-scaling of MEC curves, that is to say, for a second-order MPT, the rescaled $\Delta S'_M$ curves should collapse into a single curve independent of the external magnetic field and temperature; however, for a first-order one, the rescaled $\Delta S'_M$ curves should display a dispersive behavior. Franco's universal curves can be constructed by (1) normalizing each $\Delta S_M(T)$ curve with its respective maximum value $\Delta S_M{}^{max}$ (i.e., $\Delta S' = \Delta S_M(T)/\Delta S_M{}^{max}$) and (2) the temperature axis is rescaled by a new variable, θ, defined by the following expression [34]:

$$\theta = \begin{cases} -(T - T_C)/(T_1 - T_C) & T \le T_C \\ (T - T_C)/(T_2 - T_C) & T > T_C \end{cases} \quad (6)$$

where T_{r1} (below T_C) and T_{r2} (above T_C) are two reference temperatures, which can be selected for each curve from temperature corresponding to $\Delta S_M(T_{r1})/\Delta S_M{}^{max} = \Delta S_M(T_{r2})/\Delta S_M{}^{max} = 0.5$.

Figure 6 shows the universal curves by plotting $\Delta S'$ against θ for the $La_{0.9}Sb_{0.1}MnO_3$ compound. One can clearly find out from this figure that all the rescaled $-\Delta S_M$ curves under different magnetic field changes collapse onto a single universal curve, which confirms that the FM-PM transition of $La_{0.9}Sb_{0.1}MnO_3$ is second order.

3.5 The Temperature Dependence of MEC

In this section, we will model the experimental values of $-\Delta S_M$ using Lauder's theory to study the contributions in the MCE of the $La_{0.9}Sb_{0.1}MnO_3$ compound. Based on this theory, the magnetic energy can be included in expression of

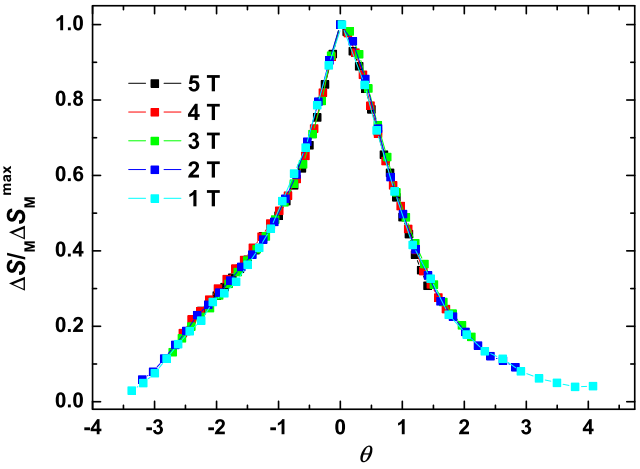

Fig. 6 Normalized MEC ($\Delta S_M/\Delta S_M{}^{max}$) as a function of the rescaled temperature θ for different applied fields for $La_{0.9}Sb_{0.1}MnO_3$

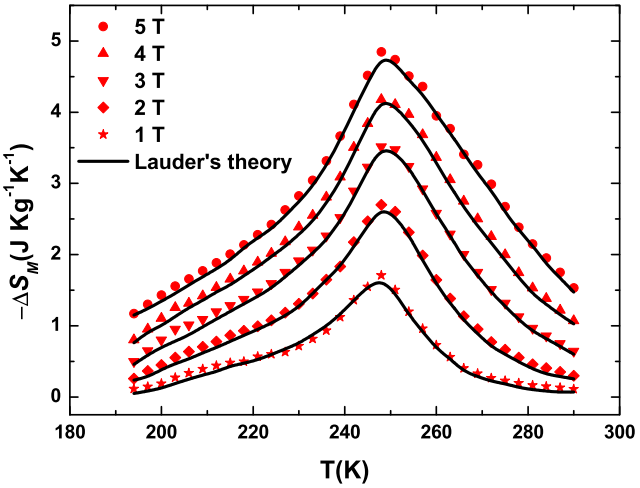

Fig. 8 Experimental and theoretical MEC for $La_{0.9}Sb_{0.1}MnO_3$ for $\mu_0 H = 1$–5 T

Gibb's free energy [35]. Neglecting the higher-order parts, Gibb's free energy can be written as in Eq. 7,

$$G(T, M) = G_0 + \frac{1}{2}A(T)M^2 + \frac{1}{4}B(T)M^4 - MH \qquad (7)$$

where $A(T)$ and $B(T)$ are well known as Lauder coefficients, which are temperature-dependent parameters standing for the magneto-elastic coupling and electron condensation energy [35], and can be obtained at the equilibrium state of $\partial G/\partial M = 0$

$$\frac{H}{M} = A(T) + B(T)M^2 \qquad (8)$$

The values of $A(T)$ and $B(T)$ can be obtained from the linear region of the Arrott plots by a polynomial fitting. The values of Landau coefficients $A(T)$ and $B(T)$ as functions of the temperature are plotted in Fig. 7. Parameter $A(T)$ is observed to be almost linear for $La_{0.9}Sb_{0.1}MnO_3$, whereas the temperature dependence of $B(T)$ is highly nonlinear. In principle, parameter $B(T)$ plays a key role in determining

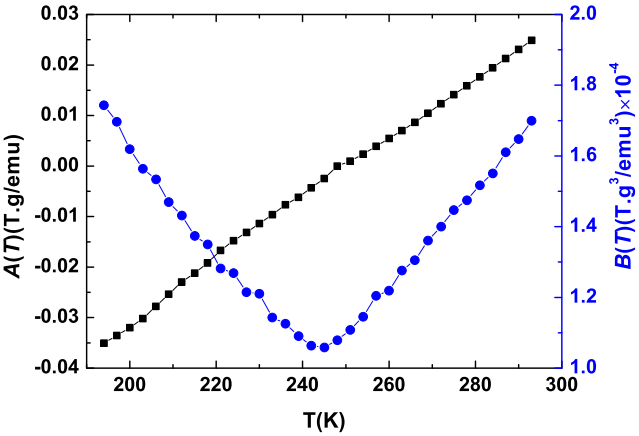

Fig. 7 The temperature dependence of Lauder's coefficients $A(T)$ and $B(T)$

the order of MPT. Amaral et al. [35] have found that $B(T_C)$ can be positive, zero, or negative. If $B(T_C) > 0$, the MPT is of the second order; otherwise, it is of the first order. It is clear from this figure that $B(T_C)$ is positive, implying that the MPT of $La_{0.9}Sb_{0.1}MnO_3$ belongs to the second order.

The temperature dependence of MEC is theoretically determined from differentiation of the magnetic part of the free energy and can be written as follows [36]:

$$S_M(T, H) = -\frac{1}{2}\frac{\partial A(T)}{\partial T}M^2 - \frac{1}{4}\frac{\partial B(T)}{\partial T}M^4 \qquad (9)$$

With the values of $A(T)$ and $B(T)$ extracted from the data, the variation of the experimental and estimated MEC versus temperature at some fields (1–5 T in this work) for $La_{0.9}Sb_{0.1}MnO_3$ are shown in Fig. 8. An excellent agreement is observed between the experimental data and the one calculated by Lauder's theory. The present analysis further proves the important role of both magneto-elastic coupling and the electron interaction in the study of the MCE of electron-doped $La_{0.9}Sb_{0.1}MnO_3$ manganite.

4 Conclusions

We prepared an electron-doped $La_{0.9}Sb_{0.1}MnO_3$ polycrystalline compound using the sol-gel method and then investigated its MCE and MPT. XRD pattern shows that the material crystallized in a rhombohedral structure with the $R\bar{3}C$ space group. This sample shows a FM-PM transition at $T_C = 248$ K. A maximum MEC of 4.79 J kg^{-1} K^{-1} and a RCP of 258.15 J kg^{-1} are observed at $\mu_0 H = 5$ T. The values of $-\Delta S_M{}^{max}$ are comparable to some hole-doped manganese compounds. However, the RCP value of $La_{0.9}Sb_{0.1}MnO_3$ is much higher than that of some hole-doped manganites under the same field change. These results suggest that

the $La_{0.9}Sb_{0.1}MnO_3$ compound is a proper candidate material for magnetic refrigerators near sub-room temperature. Both Arrott plots and Franco's universal curves indicate that the MPT between FM and PM states is of the second order. Moreover, the temperature dependence of the MEC can be well understood within the framework of Lauder's theory.

Acknowledgments This work is supported by the National Natural Science Foundation of China under grant no. 11605133 and the Scientific Research Program funded by ShaanXi Provincial Education Commission (Program No. 2010JK674).

References

1. Nagaev, E.L.: Phys. Rep. **346**, 387 (2001)
2. Tokura, Y.: Rep. Prog. Phys. **69**, 797 (2006)
3. Dagotto, E., Hotta, T., Moreo, A.: Phys. Rep. **344**, 1 (2001)
4. Ahmed, S.A.: J. Magn. Magn. Mater. **340**, 131 (2013)
5. Kansara, S.B., Dhruv, D., Kataria, B., Thaker, C.M., Rayaprol, S., Prajapat, C.L., Singh, M.R., Solanki, P.S., Kuberkar, D.G., Shah, N.A.: Ceram. Int. **41**, 7162 (2015)
6. Juan, Z., Lirong, L., Gui, W.: Adv. Powder Technol. **22**, 68 (2011)
7. Tan, G.T., Dai, S.Y., Duan, P., Zhou, Y.L., Lu, H.B., Chen, Z.H.: Phys. Rev. B **68**, 014426 (2003)
8. Shelke, A.R., Ghodake, G.S., Kim, D.Y., Ghule, A.V., Kaushik, S.D., Lokhande, C.D., Deshpande, N.G.: Ceram. Int. **42**, 12038 (2016)
9. Kumar, N., Tripathi, R., Dogra, A., Awana, V.P.S., Kishan, H.: J. Alloys and Compd. **492**, L28 (2010)
10. Gao, J., Wang, L.: Mater. Sci. Eng. B **144**, 97 (2007)
11. Duan, P., Dai, S.Y., Tan, G.T., Lu, H.B., Zhou, Y.L., Cheng, B.L., Chen, Z.H.: J. Appl. Phys. **95**, 5666 (2004)
12. Zener, C.: Phy. Rev. **81**, 440 (1951)
13. Yang, J., Sun, Y.P., Sun, W.H., Lee, Y.P.: J. Appl. Phys. **100**, 123701 (2006)
14. Mahato, R.N., Sethupathi, K., Sankaranarayanan, V., Nirmala, R.: J. Magn. Magn. Mater. **322**, 2537 (2010)
15. Shelke, A.R., Ghule, A.V., Lee, Y.P., Lokhande, C.D., Deshpande, N.G.: J. Alloys Compd. **692**, 522 (2017)
16. Wang, D., Wang, M., Wang, R., Li, Y.: J. Rare Earths **31**, 257 (2013)
17. Duan, P., Tan, G.T., Dai, S.Y., Zhou, Y.L., Chen, Z.H.: J. Phys.: Condens. Matter **15**, 4469 (2003)
18. Venkataiah, G., Huang, J.C.A., Venugopal Reddy, P.: J. Alloys Compd. **562**, 128 (2013)
19. Bohigas, X., Tejada, J., Del Barco, E., Zhang, X.X., Sales, M.: Appl. Phys. Lett. **73**, 390 (1998)
20. Anwar, M.S., Kumar, S., Ahmed, F., Arshi, N., Koo, B.H.: Mater. Res. Bull. **47**, 2977 (2012)
21. Abassi, M., Dhahri, N., Dhahri, J., Hlil, E.K.: Phys. B **449**, 138 (2014)
22. Wada, H., Tanabe, Y.: Appl. Phys. Lett. **79**, 3302 (2001)
23. Phan, M.H., Yu, S.C.: J. Magn. Magn. Mater. **308**, 325 (2007)
24. Gschneidner Jr., K.A., Pecharsky, V.K., Tsokol, A.O.: Rep. Prog. Phys. **68**, 1479 (2005)
25. Rostamnejadi, A., Venkatesan, M., Kameli, P., Salamati, H., Coey, J.M.D.: J. Magn. Magn. Mater. **323**, 2214 (2011)
26. Morelli, D.T., Mance, A.M., Mantese, J.V., Micheli, A.L.: J. Appl. Phys. **79**, 373 (1997)
27. Min, S.G., Kim, K.S., Yu, S.C., Suh, H.S., Lee, S.W.: IEEE Trans. Magn. **41**, 2760 (2005)
28. Kolat, V.S., Atalay, S., Izgi, T., Gencer, H.: Metall. Mater. Trans. A **46A**, 2591 (2015)
29. Guo, Z.B., Du, Y.W., Zhu, J.S., Huang, H., Ding, W.P., Feng, D.: Phys. Rev. Lett. **78**, 1142 (1997)
30. Pecharsky, V.K., Gschneidner Jr., K.A.: Phys. Rev. Lett. **78**, 4494 (1997)
31. Banerjee, S.K.: Phys. Lett. **12**, 16 (1964)
32. Franco, V., Conde, A., Romero-Enrique, J.M., Blazquez, J.S.: J. Phys.: Condes. Matter **20**, 285207 (2008)
33. Bonilla, C.M., Bartolome, F., Garcia, L.M., Parra-Borderias, M., Herrero-Albillos, J., Franco, V.: J. Appl. Phys. **107**, 09E131 (2010)
34. Franco, V., Conde, A., Pecharsky, V.K., Gschneidner Jr., K.A.: Europhys. Lett. **79**, 47009 (2007)
35. Amaral, V.S., Amaral, J.S.: J. Magn. Magn. Mater. **272**, 2104 (2004)
36. Kallel, S., Kallel, N., Pena, O., Oumezzine, M.: Mater. Lett. **64**, 1045 (2010)